Theoretical Elucidation of a Classic Reaction: Protonation of the Quadruple Bond of the Octachlorodimolybdate(II,II) [Mo$_2$Cl$_8$]$^{4−}$ Anion

Emmanuel D. Simandiras,*,† Metaxia Tsakiroglou,† Nikolaos Psaroudakis,‡ Dimitrios G. Liakos,†,§ and Konstantinos Mertis‡

†Theoretical and Physical Chemistry Institute, National Hellenic Research Foundation, 48 Vassileos Constantinou Avenue, 116 35 Athens, Greece

‡Inorganic Chemistry Laboratory, Department of Chemistry, University of Athens, Panepistimiopolis Zografou, 157 71 Athens, Greece
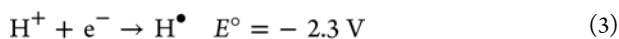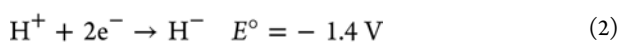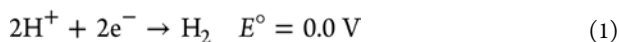
Ⓢ Supporting Information

ABSTRACT: The protonation reaction of the unbridged quadruple metal−metal bond of [Mo$_2$Cl$_8$]$^{4−}$ anion producing the triply bonded hydride [Mo$_2(\mu$-H$)(\mu$-Cl$)_2$Cl$_6$]$^{3−}$ is studied by accurate Density Functional Theory computations. The reactant, product, stable intermediates, and transition states are located on the potential energy surface. The water solvent is explicitly included in the calculations. Full reaction profiles are calculated and compared to experimental data. The mechanism of the reaction is fully elucidated. This involves two steps. The first is a proton transfer from an oxonium ion to the quadruple bond, being rate determining. The second, involves the internal rearrangement of chlorine atoms and is much faster. Activation energies with a mean value of 19 kcal/mol are calculated, in excellent agreement with experimental values.
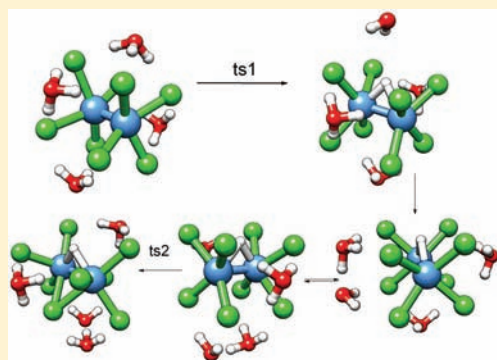
■ INTRODUCTION

The reduction of protons as the initial step toward dihydrogen formation (eq 1) is one of the most fundamental redox transformations and a reaction of great chemical and biochemical importance.[1] The reaction although seemingly simple is complex because

(i) "H⁺" may be quite different species depending on solvent and concentration and

(ii) the reaction is bielectronic (eq 2[2]), whereas the intermediate hydrogen radical is a high energy species which practically excludes the possibility of reduction of protons via eq 3[2] unless radical stabilizers are available.

$$2H^+ + 2e^- \rightarrow H_2 \quad E° = 0.0 \text{ V} \quad (1)$$

$$H^+ + 2e^- \rightarrow H^- \quad E° = -1.4 \text{ V} \quad (2)$$

$$H^+ + e^- \rightarrow H^\bullet \quad E° = -2.3 \text{ V} \quad (3)$$

Essential to all catalytic systems seems to be the binding of protons to a Brönsted base followed by liberation of H$_2$ by several possible ways. Transition metal complexes can act as proton acceptors uniquely combining Brönsted base properties with redox activity.

Metal centers of the majority of low valent mononuclear complexes can function in such a way, being amenable to protonation, although the corresponding acids may not be always isolable. Most interestingly, the M−M bonds in binuclear complexes can be as basic as weak amines,[3] and also, in certain cases were shown to be substantially higher than that of the metal sites in related 18e mononuclear complexes or even to the basic sites of the ancillary ligands.[4] As a result, metal−metal bonds readily can be protonated to form hydride bridged species.[5]

The Ni−Fe bonds in hydrogenases (H$_2$ ⇌ 2H⁺ + 2e⁻) are likely sites for protonation to form a bridging hydride as the initial step of H$_2$ formation.[1a] Theoretical studies of NiFe hydrogenase mechanism indicate that hydride bridged intermediates are energetically favorable.[6] In the case of Fe−Fe hydrogenases, a terminal hydride is involved.[7]

A coordination complex that has attracted attention in the context of proton reduction catalysis is [Mo$_2$Cl$_8$]$^{4−}$. The anion undergoes slow protonation with concentrated hydrochloric acid, giving the bridging hydride [Mo$_2(\mu$-H$)(\mu$-Cl$)_2$Cl$_6$]$^{3−}$ (eq 4) with the reaction constituting the first example of an oxidative addition involving a well-defined metal−metal bond.[8] The kinetics of the reaction in aqueous HCl has been shown to obey a linear dependence with respect to the acidity function.[9]

$$[Mo_2Cl_8]^{4-} + H^+ \rightarrow [Mo_2Cl_8H]^{3-} \quad (4)$$

The theoretical study of metal−metal multiple bonds (order four or higher) has become of increasing interest in recent years because of the advances of Density Functional Theory and of wave function methods that include electron correlation. A recent benchmark study on quadruple metal−metal bonds[10] covers a number of compounds involving Tc, Re, Ru, Os, Rh, and Ir but not $[Mo_2Cl_8]^{4-}$. (See also their references for a few other recent studies of order four or higher metal−metal bonds, mainly of Cr, Re, and U). The multiconfigurational CASPT2 method has also been used for the study of quadruply bonded metal dimers.[11]

Takagi, Krapp, and Frenking[10] find that a number of DFT functionals are from adequate to quite good in the description of metal−metal quadruple bonds and corresponding energies, the generalized gradient approach (GGA) functionals being the most accurate. To our knowledge, no recent theoretical study of $[Mo_2Cl_8]^{4-}$ has been reported, with the exception of the 1974 Xα computation of Norman and Kolari;[12] using the crystallographic parameters of Brencic and Cotton,[13] they perform an electronic structure calculation at the SCF-Xα level, which produces a good representation of the $\sigma^2\pi^4\delta^2$ bonding picture and an explanation of the electronic spectrum.

A further point that needs to be addressed is that the reaction under study here takes place in aqueous solution. Continuum solvation models have proven very efficient in a great number of theoretical studies and are reviewed extensively.[14] In this case, however, a more realistic approach will be necessary. Discrete solvation methods have been used for some accurate studies of processes involving transition metals; a review is given by Hush, Schamberger, and Bacskay[15] for *cis*- and *trans*-platinum chloride, and also a more recent study of Truhlar and co-workers[16] utilizes discrete solvation for the determination of the Ru^{3+}/Ru^{2+} reduction potential. However, studies with explicit inclusion of the solvent molecules in the study of reaction mechanisms involving transition metals are scarce, if any.

COMPUTATIONAL DETAILS

The Density Functional Theory (DFT) method was used for all calculations, employing three different functionals; the hybrid B3LYP (Becke−Lee−Yang−Parr),[17] the generalized gradient nonempirical PBE,[18] and B97D, a nonempirical functional due to Grimme.[19] The first was chosen because of its popularity and overall accuracy, the second following the findings of Takagi et al[10] that show a very good performance of GGA functionals and especially PBE for quadruple metal−metal bonds, and the third because it includes approximate dispersion effects. All methods were used as implemented in the Gaussian 09 suite of programs,[20] which was used for all computations. Average solvent effects were added with the Integral Equation Formalism Polarizable Contiuum Model (IEFPCM) due to Tomasi and co-workers[14] as implemented in Gaussian09.

The basis set used throughout is the triple-ζ quality basis because of Weigend and Ahlrichs[21] denoted as def2-TZVPP including an Effective Core Potential to account for the core and average relativistic effects.[22] Only in the initial search for structures of the complexes with oxonia and water molecules the smaller def2-SVP basis[21,22] was used.

The investigation of a reaction mechanism involves the location of stable intermediates, as well as transition states of the potential energy surface. For this investigation, the same methodology was used throughout; full structure optimizations were performed using standard and in some cases tight criteria and ultrafine integral grid. For each stationary point reached, a full analytical force constant calculation was used to ensure a local minimum (no negative eigenvalues) or a transition state (one negative eigenvalue).
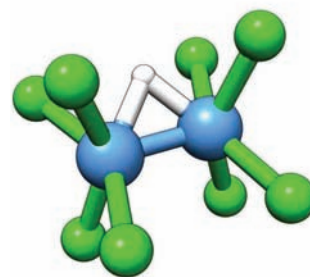
RESULTS AND DISCUSSION

i. $[Mo_2Cl_8]^{4-}$ Structure. The structure of the octachlorodimolybdate(II,II) ion $[Mo_2Cl_8]^{4-}$ was fully optimized using both DFT functionals, B3LYP and PBE, and frequencies were calculated at the minimum of the potential energy surface. The structure is shown in Figure 1a and basic
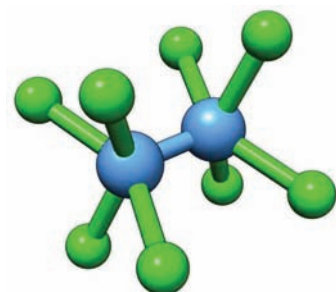
a. Structure of $[Mo_2Cl_8]^{4-}$
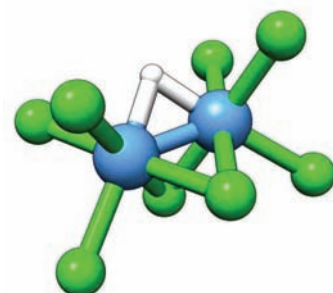
b. Structure of $[Mo_2(\mu\text{-}H)(\mu\text{-}Cl)_2Cl_6]^{3-}$

c. Structure of $[Mo_2(\mu\text{-}H)Cl_8]^{3-}$

Figure 1. Structure of $[Mo_2Cl_8]^{4-}$, structure of $[Mo_2(\mu\text{-}H)(\mu\text{-}Cl)_2Cl_6]^{3-}$, and the stable intermediate.

geometrical parameters are tabulated in Table 1 and compared to the crystallographic data obtained by Brencic and Cotton in

Table 1. Calculated and Experimental Structure of $[Mo_2Cl_8]^{4-}$ (Å and deg)

	$r(Mo−Mo)$	$r(Mo−Cl)$	$\theta(Mo−Mo−Cl)$
B3LYP	2.094	2.580	109.0
PBE	2.131	2.550	108.3
Expt	2.14	2.45	105

1970.[13] To our knowledge, no newer experimental or theoretical determination of the structure of this ion has been reported.

Table 2. Structure and Vibrational Frequencies of $[Mo_2(\mu\text{-}H)(\mu\text{-}Cl)_2Cl_6]^{3-}$ (Å and deg)

	Mo–Mo	Mo–H	Mo–Cl$_{bridge}$	Mo–Cl$_{transH}$	Mo–Cl$_{transCl}$	Mo–H–Mo	ν_1	ν_2
PBE	2.279	1.813	2.534	2.557	2.445	77.9	1252	1621
B3LYP	2.246	1.805	2.550	2.582	2.463	77.0	1223	1669
X-ray[8]	2.376	1.73	2.478	2.498	2.394	86		
neutron[8]	2.357	1.823	2.486	2.490	2.401	80.6		
expt[24]							1248–1270	1553–1580

Given the difference that exists between the crystallographic and theoretical data (theory is for an isolated molecule with no vibrational averaging, whereas in the crystallographic data the lattice effects are significant) and the large error bars that were associated with the experimental data, the agreement especially of the multiple metal–metal bond length is very good. As was reported in an extensive recent study[10] of quadruple metal–metal bonds, the generalized gradient approximation functional PBE is overall more accurate in describing the quadruple bonding, however B3LYP, which is a widely used functional does not differ significantly and is also reasonably accurate.

Both theoretical methods describe correctly the quadruple bond and the $\sigma^2\pi^4\delta^2$ configuration. A further confirmation of the accurate description of this molecule is the accuracy in the determination of the vibrational frequencies, as shown by the excellent agreement achieved especially by the PBE functional. The Mo–Mo stretching frequency was determined from Raman spectroscopy[23] to be 347.1 ± 0.5 cm^{-1} with very low anharmonicity, and the DFT/PBE harmonic value found is 354 cm^{-1}. B3LYP is also found to be quite close at 378 cm^{-1}. Further calculated frequencies are found at 220 cm^{-1} (182km/mol) for the doubly degenerate symmetric Mo–Cl stretch and 207 cm^{-1} (107 km/mol) for the asymmetric Mo–Cl stretch.

ii. $[Mo_2(\mu\text{-}H)(\mu\text{-}Cl)_2Cl_6]^{3-}$ Structure. The structure of $[Mo_2(\mu\text{-}H)(\mu\text{-}Cl)_2Cl_6]^{3-}$ was also fully optimized with both functionals, and a full vibrational analysis was performed. It is found that the Mo–Mo bond length is consistently elongated for both B3LYP and PBE (see below). The structure of $[Mo_2(\mu\text{-}H)(\mu\text{-}Cl)_2Cl_6]^{3-}$ is shown in Figure 1b and the basic geometrical and vibrational data are compared in Table 2. This molecule has been studied experimentally, X-ray and neutron scattering structure data being available,[8] as well as solid state IR spectroscopic data.[24] A theoretical Xα calculation by Bino et al.[25] has also been reported, where the strength of the Mo–H–Mo interaction was analyzed.

In Table 2, Cl$_{bridge}$ refers to a bridging Cl atom, Cl$_{transH}$ to a Cl atom trans to the bridging H atom and Cl$_{transCl}$ to a Cl atom trans to the bridging and remaining Cl atoms. A very good overall agreement of experimental and theoretical data is noted, especially bearing in mind that experimental data are obtained from the solid state and carry relatively large error bars. It is of particular interest to note that the ordering of Mo–Cl bonds is reproduced by the theory, namely Mo–Cl$_{transH}$ > Mo–Cl$_{bridge}$ ≫ Mo–Cl$_{transCl}$.

The elongation of the quadruple metal–metal bond after protonation is a matter of interest, and in some cases, the results are counterintuitive.[26] The results of Tables 1 and 2 show that theory correctly predicts the elongation of the Mo–Mo bond upon protonation, although not to the full extent suggested by experimental results, which, however, bear significantly different error bars. The B3LYP elongation is 0.152 Å, and the PBE is 0.148 Å, the X-ray being 0.236 Å. Test multiconfigurational CASSCF calculations were performed for $[Mo_2(\mu\text{-}H)(\mu\text{-}Cl)_2Cl_6]^{3-}$ showing that the system is well

described by a single configuration, the separation from the lowest triplet being found in the order of 4000 cm^{-1}. The small difference in the elongation can therefore be attributed to the inability of a gas phase calculation to reproduce solid state data in greater accuracy, as well as the limitations of the basis set and the method.

In their Xα study, Bino et al[25] analyze the Mo–H–Mo interaction and find a strong three center four electron interaction that is divorced from all the Mo–Cl interactions. In particular, they find an a$_1$ orbital that is 27 below the HOMO and that is roughly equally Mo and H in character, and they attribute the strength of the Mo–H–Mo interaction to this orbital in conjunction to the HOMO, which is mainly Mo in character. Our DFT data, both with B3LYP and PBE support and further clarify this. Indeed, a HOMO-27 a$_1$ orbital is found which contains strong Mo–H interactions, but almost no direct Mo–Mo interaction. Simultaneously, the HOMO a$_1$ has strong Mo–Mo interaction, but also a significant overlap with H. These two orbitals constitute the three center four electron bond. Further, the HOMO-1 and HOMO-2 orbitals retain a lot of their original π and σ character, respectively, from the unprotonated species, and have little Mo–H interaction. The above orbitals have essentially no interaction with Cl atoms; however, the HOMO-7 shows a small interaction between the bridging Cl and H.

The theoretical vibrational frequencies given here are only the two that are directly compared to the measured data, and are described as the movement of the bridging hydrogen parallel (ν1) and perpendicular (ν2) to the triple bond. A good agreement is seen, especially in ν_1. The calculated intensities are 293 and 16 km/mol, respectively, also in agreement with the measured spectrum, in which the second is given as medium and the first as very strong. Further calculated frequencies are found to be the various Mo–Cl stretches at 306(136), 281(26), 263(86), 258(97), 243(29), 229(134), and 195(17) cm^{-1}(intensity in km/mol). Worth noting is that the Mo–Mo stretch is found to be at 354 cm^{-1} virtually unchanged compared to $[Mo_2Cl_8]^{4-}$, the difference being that it is now IR active with an intensity of 12 km/mol.

From the above discussion, it is quite clear that the theoretical methods employed accurately describe both the reactant $[Mo_2Cl_8]^{4-}$ and the product $[Mo_2(\mu\text{-}H)(\mu\text{-}Cl)_2Cl_6]^{3-}$ molecules, and it is therefore correct to proceed to the investigation of the reaction mechanism with the methods described.

iii. Reaction Mechanism with No Solvent Involved. The reaction mechanism was initially investigated for the isolated molecules, omitting any interaction to solvent or other molecules in the liquid environment.

By approaching a proton perpendicular to the quadruple bond of $[Mo_2Cl_8]^{4-}$, it is found that this readily attaches to the side of the molecule as bridging hydrogen. This happens in a barrierless fashion; in fact the energy lowering is quite significant due to the 4– charge of the reactant. This H bridged

intermediate structure with no bridging chlorine atoms and an overall charge of 3−, is found to be stable local minimum of the potential energy surface. This intermediate was first postulated by Miller and Haim[9] but has never been, to our knowledge, isolated or theoretically studied. This therefore is the first observation of $[Mo_2(\mu\text{-}H)Cl_8]^{3-}$; it was therefore fully optimized and its structure and IR spectrum were calculated. The structure is shown in Figure 1c; at the PBE level, the Mo−Mo bond is found to be 2.270 Å (0.009 Å shorter compared to $[Mo_2(\mu\text{-}H)(\mu\text{-}Cl)_2Cl_6]^{3-}$), the Mo−H 1.802 Å (0.011 shorter), and the Mo−H−Mo angle virtually unchanged at 78°. The Mo−Cl bonds are all 2.468 Å on the hydrogen side and 2.439 Å on the other side. The ν_1 and ν_2 vibrational frequencies (intensities in parentheses) are 1215 (95) and 1629 (1) cm^{-1} (km/mol), respectively. The shift is not significant compared to the values for the final product as shown in Table 2, but a great decrease in the intensity is noted. A new peak appears at 696 cm^{-1} (15 km/mol) and corresponds to a third vibration of hydrogen vertical to the Mo−H−Mo plane. The Mo−Mo stretch is at 322 cm^{-1} (0.5 km/mol).

Further on the protonation mechanism, this intermediate was then found to rearrange toward the final product, via a low transition state, which is named ts2 (vide infra a ts exists in a previous step when solvent is involved, which will be named ts1). The structure of ts2 and the form of the imaginary frequency involved is shown in Figure 2b. The overall reaction is shown in Scheme 1.
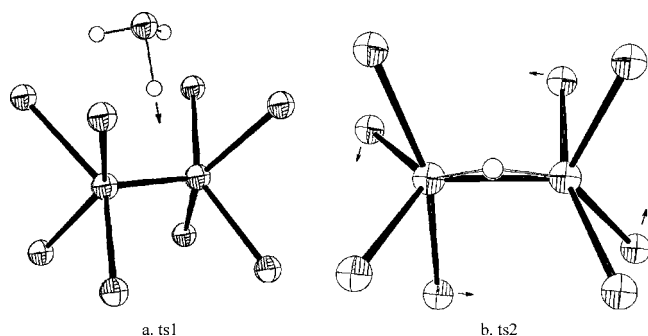
Figure 2. Two transition states; ts2 is a top view, and the arrows are on the lower Cl atoms.

The total energies for reactant, stable intermediate, ts2 and product are given in Table 3, both at the equilibrium position for the corresponding structure and at the vibrationally averaged $v = 0$ level, for both functionals. The corresponding reaction profile is shown in Figure 3. Examination of this profile shows that the protonation reaction in the gas phase would proceed with virtually no barrier and great stabilization toward $[Mo_2(\mu\text{-}H)(\mu\text{-}Cl)_2Cl_6]^{3-}$. This, however, is not found to be the case from the experimental data obtained in solution.[9,27] It is therefore absolutely necessary to simulate the true reaction environment as closely as possible in order to explain the measured reaction barrier.

iv. Reaction Mechanism with One Water Molecule. As seen in the previous section, the approach of H$^+$ to the quadruple bond is clearly not realistic enough for an exact theoretical investigation of the reaction in solution. In a first step toward a more elaborate approach, we replace the bare proton by an oxonium ion $[H_3O]^+$. This is found to attach to the $[Mo_2Cl_8]^{4-}$ ion again in a very exothermic complex
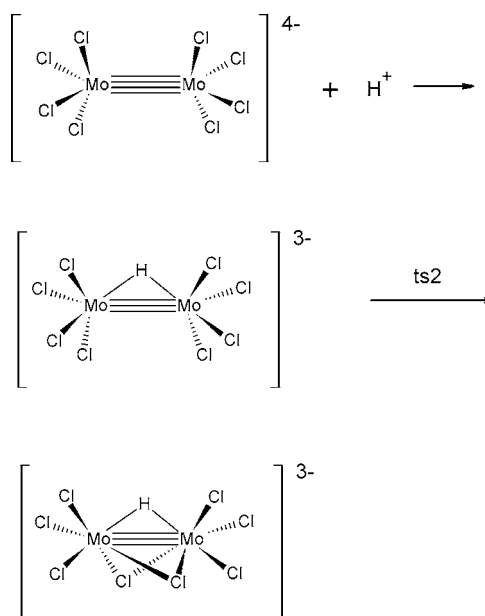
Scheme 1

Table 3. Relative Energies (in kcal/mol, Relative to the Protonated Intermediate) of Compounds of Scheme 1

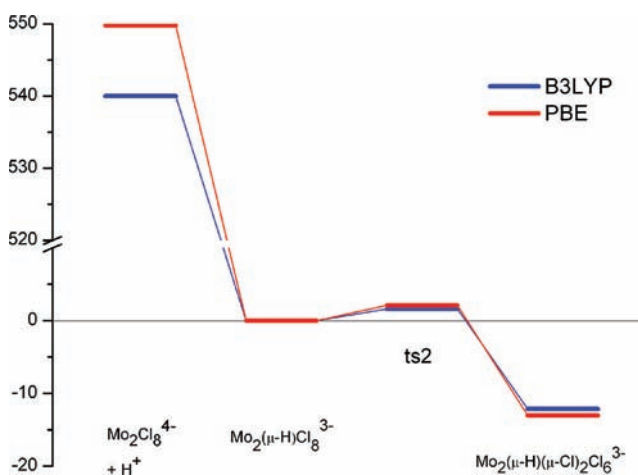| compound	B3LYP	B3LYP ($v = 0$)	PBE	PBE ($v = 0$)
$Mo_2Cl_8^{4-}$ + H$^+$	540.0	534.0	549.8	543.9
$Mo_2(\mu\text{-}H)Cl_8^{3-}$	0.0	0.0	0.0	0.0
ts2	1.6	1.5	2.1	2.0
$Mo_2(\mu\text{-}H)(\mu\text{-}Cl)_2Cl_6^{3-}$	−12.2	−12.1	−13.0	−12.9

Figure 3. Reaction profile of Scheme 1 (energy in kcal/mol).

formation that leads to an intermediate stable structure pictured in Scheme 2.

From this stable $[(Mo_2Cl_8)\cdot(H_3O)]^{3-}$ complex, a transition state was located that corresponds to the movement of the proton of the oxonium ion toward the quadruple bond, leading to the formation of the H-bridged stable intermediate discussed in the previous section. This transition state is labeled ts1 with its structure shown in Figure 2a. The corresponding energies are given in Table 4, and a reaction profile is available as Supporting Information.
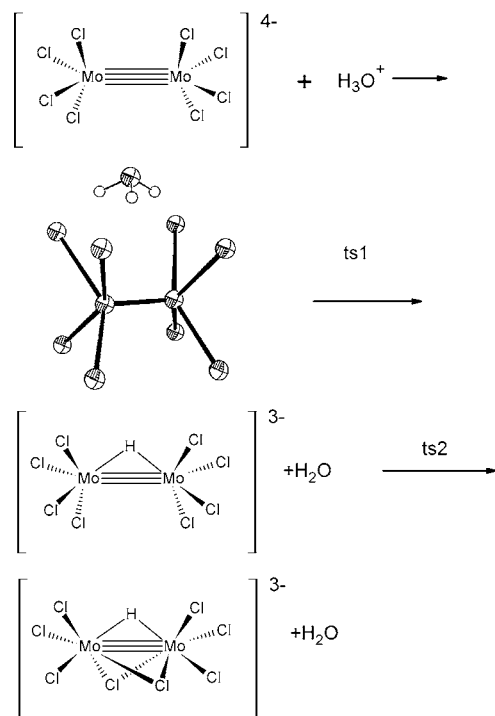
Scheme 2

Table 4. Relative Energies (in kcal/mol, Relative to the Oxonium Complex) of Compounds of Scheme 2

compound	B3LYP	B3LYP ($v = 0$)
$Mo_2Cl_8^{4-} + H_3O^+$	375.3	373.5
$Mo_2Cl_8^{4-} \cdot H_3O^+$	0.0	0.0
ts1	19.9	17.6
$Mo_2(\mu\text{-}H)Cl_8^{3-} + H_2O$	6.6	3.6

An activation energy of 17.6 and 19.9 kcal/mol is found, with B3LYP at the $v = 0$ and equilibrium levels respectively. This activation energy is now much more promising compared to the experimental data,[9,27] showing that the oxonium approach is in principle correct. It is therefore investigated further in the next section.

v. Reaction Mechanism in Oxonium Environment. The single oxonium ion approach improved upon the first approximation, since a two stage mechanism with activation energies of 19.9 and 1.6 kcal/mol, respectively, was found, the first being the rate determining step and in the correct order of magnitude compared to experiment. It is necessary, however, to improve the realism of the model and determine if the same two step mechanism is confirmed in a more complete solvent environment.

The following approach was chosen as a realistic model of the reaction in solution: since the reaction takes place in 6 M HCl solution, a great number of oxonium ions is expected to be present, and these will be attracted by the negatively charged $[Mo_2Cl_8]^{4-}$; a number of oxonium ions will therefore be added in an aggregate surrounding the central ion. The choice of the number of oxonium ions that will be used in the study to obtain the best balance between efficiency and accuracy is rather arbitrary, but four appears to be suitable so as to match the initial formal charge of $[Mo_2Cl_8]^{4-}$ giving a neutral cluster. This is then treated in an average solution environment with the

PCM method. Further Cl$^-$ are not involved in the mechanism at this stage. The $[(Mo_2Cl_8) \cdot (H_3O)_4]$ cluster is treated with both DFT functionals, and the reaction mechanism is summarized in Scheme 3 and will be discussed here.

The first step involves the full geometry optimization of the $[(Mo_2Cl_8) \cdot (H_3O)_4]$ cluster, using various initial geometries corresponding to different arrangements of the four oxonia around the central ion. From a number of stable structures found from many starting points involving all possible positions, the one that is clearly lowest in energy and therefore favored is the one shown as the starting figure in Scheme 3 which will be labeled henceforth **1**. In this structure, the four oxonia are arranged on the four sides of the quadruple bond, which is lengthened by 0.008–2.139 Å with the PBE functional. All Mo−Cl bonds are lengthened and the symmetry is broken; these are now 2.429, 2.436, 2.512, and 2.525 Å from each molybdenum atom. The metal−metal bond remains formally quadruple with no significant change to the orbitals. The stability of this complex is confirmed by the fact that the lowest vibrational frequency involving movement of oxonium ions is 61 cm^{-1}. The Mo−Mo stretching frequency is calculated at the PBE level to be 363 cm^{-1}, a shift of 9 cm^{-1} compared to the free molecule.

Further in the protonation reaction, a transition state similar to the one described above was then located. This is very similar to the one shown in Figure 2a and labeled again ts1, as it is essentially equivalent with the ts1 of the previous section, the difference being that three further oxonia are attached to the molecule. The imaginary frequency of ts1 is 866 cm^{-1} and corresponds to detachment of one proton from the oxonium ion and attachment as a bridging hydrogen of the central ion. The arrow shown in Figure 2a corresponds to this imaginary frequency.

A complete list of relative energies for the reaction of Scheme 3 at all levels of theory is given in Table 5, where the energy of the stable $[(Mo_2Cl_8) \cdot (H_3O)_4]$ cluster is taken as zero. From this table, it is seen that the barrier calculated for the first reaction step varies between 13.8 and 23.9 kcal/mol for the various methods, in excellent agreement with Mertis et al.[27] who find a barrier of 19.2 kcal/mol. The relatively small (0.7 kcal/mol) effect of the continuum solvent environment is noted, meaning that most of the solvent effect has been already included by the discrete solvation, as well as the agreement between all functionals, including B97D with dispersion corrections. It can therefore be claimed that the prediction is accurate within the range of about 10 kcal/mol given above.

The transition state ts1 further goes toward a stable intermediate structure where one oxonium is broken, and its proton is inserted as bridging hydrogen, the water molecule being left loosely attached on two chlorine atoms. The lower chlorine atoms have not yet rearranged toward bridging positions. The structure of this intermediate is the second shown in Scheme 3 and will be labeled **2.1**.

At this stage it is reasonable to expect that there will be other more favorable positions for the water molecule (from which a proton was detached) to attach to the central molecule. Of course there are more water molecules surrounding the cluster, so it is not possible to determine if the same molecule will migrate or if it will be exchanged from one coming from the environment. In any case, test calculations showed that the same water molecule can move between different positions in the cluster with a very low barrier of a few kcalories per mole.
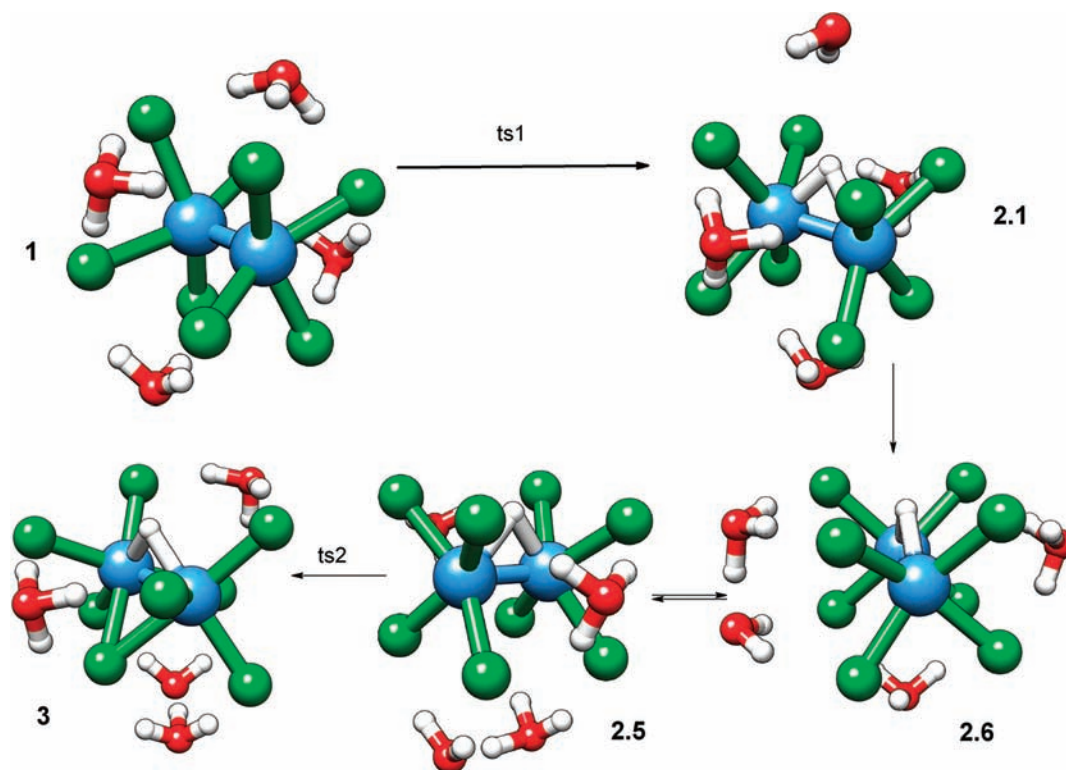
Scheme 3

Table 5. Relative Energies (in kcal/mol, Relative to 1) for the Reactants, Transition States, Intermediates, and Products of the Reaction Using Various Functionals for DFT[a]

compound	B3LYP	B3LYP ($v = 0$)	B3LYP solvent	B3LYP solvent ($v = 0$)	PBE	PBE ($v = 0$)	B97D	B97D ($v = 0$)
1	0.0	0.0	0.0	0.0	0.0	0.0	0.0	0.0
ts1	23.2	19.7	23.9	19.9	16.9	13.8	21.3	17.8
2.1	12.7	9.7	9.0	5.5	10.6	8.1		
2.6	−1.3	−2.8			−3.5	−4.6		
2.5	−0.4	−2.5	−0.8	−3.8	−3.0	−4.8		
ts2	2.7	0.4	7.4	5.5	0.7	−1.1		
3	−3.2	−5.6	2.4	0.2	−6.3	−8.4	5.2	3.0

[a]For the $v = 0$ energies, a vibrational averaging has been taken into account. All structures optimized except for the B3LYP solvent calculations.

It should be stressed at this point that the choice of the number of oxonium and water molecules surrounding $[Mo_2Cl_8]^{4-}$ is arbitrary but reasonable. Clearly, more water molecules can be attached in the first sphere but will make very little difference in the actual stages of the reaction. In any case, additional water molecules would most probably bind in the first sphere in axial positions at the extension of the Mo−Mo bond; this was tested in initial calculations and was found to have negligible effect. If the considerable mobility of H$_2$O around the cluster is also taken into account, which was found by test calculations resulting in extremely small barriers for changes in position, it would mean that addition of further solvent molecules would introduce unnecessary complication to the model without corresponding gain in accuracy. Since a reasonable number of oxonium ions was chosen for the close coordination to the reactant, this same number will be continued to the end so that the stoichiometry remains intact.

To investigate the reaction further, attempts were made from structure **2.1** to locate the transition state (ts2) that leads to the final product. This has not been possible due to the unfavorable positions of the solvent molecules. It was therefore considered necessary to investigate the various positions of the solvent molecules used so far, so as to locate the most favorable positions both energetically, and for the internal rearrangement. To achieve this, a smaller SVP basis set and the B3LYP functional was employed for efficiency reasons.

All possible arrangements of the existing stoichiometry (i.e., the central $[Mo_2(\mu\text{-}H)Cl_8]^{3-}$ stable intermediate, three oxonium ions and the water molecule from which the proton was detached) were examined at the DFT/B3LYP/SVP level of theory. The six lowest in energy structures are given in Table 6, where the positions are explained by Figure 4. These are labeled **2.1**−**2.6**. Both most favored structures have no water molecules on the side of the bridging hydrogen, but instead a H$_5$O$_2$ cluster either on the side (**2.6**) or under (**2.5**) the main molecule. As mentioned above, all internal movements of water or oxonium molecules are found to involve very low (if any) transition states. The same investigation with the smaller DFT/B3LYP/SVP set was repeated for the final product $[Mo_2(\mu\text{-}H)(\mu\text{-}Cl)_2Cl_6]^{3-}$ with three oxonium and one water molecules. The results are tabulated in Table 7, where structures are labeled **3.1**−**3.6** in correspondence to **2.1**−**2.6** for the

Table 6. Relative Energies of Various Structures of a Complex of $[Mo_2(\mu\text{-}H)Cl_8]^{3-}$ with Three $[H_3O]^+$ and One H_2O^a

position label	A	B	R	F	ax	energy (E_h)	relative to lowest (kcal/mol)
2.1	H₂O	H₃O⁺	H₃O⁺	H₃O⁺		−4125.26141023	16.0
2.2	H₂O·H₃O⁺	H₃O⁺			H₃O⁺	−4125.26313369	14.9
2.3	H₂O·H₃O⁺		H₃O⁺	H₃O⁺		−4125.27756647	5.9
2.4	H₂O·H₃O⁺	H₃O⁺	H₃O⁺			−4125.28389828	1.9
2.5		H₂O·H₃O⁺	H₃O⁺	H₃O⁺		−4125.28525329	1.0
2.6		H₃O⁺	H₃O⁺	H₂O·H₃O⁺		−4125.28692362	

^{a}The positions above (A), below (B), rear (R), front (F), and axial (ax) refer to Figure 4. SVP basis and B3LYP functional are used.
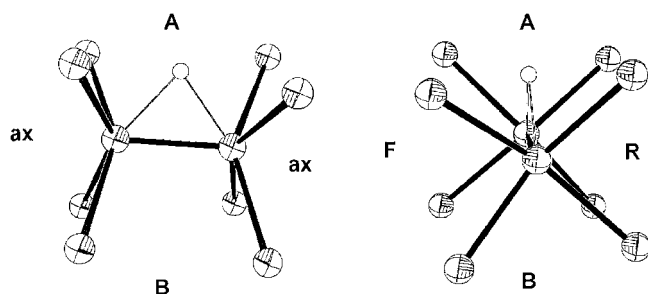

Figure 4. Positions of solvent molecules as referred in Tables 6 and 7.

intermediate. Some new structures are also added. It is noted that the most favorable structure is **3.5** corresponding to the second most favorable structure **2.5**, which is only 1 kcal/mol (at this approximate level of theory) higher than the lowest **2.6**. From **3.5**, a transition state for the rearrangement of chlorine atoms is located.

The results of this small basis investigation were then carried over to the intermediates of interest **2.1**, **2.5**, and **2.6** using the higher quality def2-TZVPP basis calculations as everywhere else in this work. The results are shown in Table 5. The initial intermediate **2.1** very easily falls (with a considerable stabilization of over 10 kcal/mol) to **2.6**. The stable intermediate **2.5** is very similar in energy to **2.6**, in most cases slightly higher as was found with the smaller basis set, but in some cases of Table 5 this is reversed. In any case **2.5** and **2.6** lie very close in energy and are very easily interchanged as in the third step of Scheme3. With the large basis set, **2.5** has again been found to correspond to a conformation that very easily rotates the lower four chlorine atoms via a transition state ts2 to give the final product. From other intermediates it has not been proven possible to locate a parallel pathway; it is therefore interesting to note that although the reaction barrier is low (in the order of 3−4 kcal/mol), only specific conformations of $[Mo_2Cl_8]^{4-}$−water−oxonium clusters will lead to that pathway.

From **2.5** via ts2 the final product which for this stoichiometry is $[(Mo_2(\mu\text{-}H)(\mu\text{-}Cl)_2Cl_6)\cdot(H_3O^+)_3\cdot(H_2O)]$ and labeled **3** is reached, with a significant stabilization. Structure **3** is similar to **3.5** from the smaller basis calculations. The transition state ts2 is similar to the one shown in Figure 2b with an oxonium molecule on each side and a $[H_5O_2]^+$ cluster rotating together with the bridging chlorine atoms. One note on the structure of ts2: at the H-bridged intermediate **2.5**, all four Mo−Mo−Cl angles for the Cl atoms opposite to the bridging H are between 100° and 105°, the small variation being due to the oxonium molecules in the environment. For ts2, the two Mo−Mo−Cl angles are about 83° and the remaining two about 125°, and for the final product **3**, the Mo−Mo−Cl angle for the bridging Cl is 64° and for the terminal Cl 130°. It is therefore seen that at ts2, the rotation of the lower Cl atoms toward the bridging position is approximately halfway completed. Finally, the activation energy for this step from Table 5 is 3.1 kcal/mol for B3LYP and 3.7 kcal/mol for PBE. It appears that the B3LYP/PCM values are larger, but one should bear in mind that the structures were not reoptimized with the IEFPCM environment.

Summarizing, it is shown that the arrangement of solvent molecules in the neighborhood of the central molecule plays a very important role in the reaction mechanism. After a proton is detached from one oxonium molecule to form a bridge, the solvent molecules are rearranged so as to lead to the pathway for the second step of the reaction. This is a realistic model of the experimental environment.

A note on PCM inclusion of outer solvent effects: from Table 5, no significant changes are induced by the addition of a water environment, even though the structures are not reoptimized. All methods and approaches support the exact same picture for the reaction; a figure where all calculations are plotted on the same axes is available as Supporting Information. It is clear that the overall picture is the same, irrespective of the method used. Dispersion effects, which were studied via B97D, only for the activation energy and the overall exothermicity, also do not alter the picture.

Table 7. Relative Energies of Various Structures of a Complex of $[Mo_2(\mu\text{-}H)(\mu\text{-}Cl)_2Cl_6]^{3-}$ with Three $[H_3O]^+$ and One H_2O^a

position label	A	B	R	F	ax	energy (E_h)	relative to lowest (kcal/mol)
3.1	H₂O	H₃O⁺	H₃O⁺	H₃O⁺		−4125.25845896	18.3
3.3	H₂O·H₃O⁺		H₃O⁺	H₃O⁺		−4125.27103507	10.4
	H₂O·H₃O⁺				H₃O·H₃O⁺	−4125.27591116	7.3
		H₃O⁺			H₂O·(H₃O⁺)₂	−4125.27809095	5.9
3.6		H₃O⁺	H₃O⁺	H₂O·H₃O⁺		−4125.28125299	4.0
3.4	H₂O·H₃O⁺	H₃O⁺	H₃O⁺			−4125.28291984	2.9
		H₂O·H₃O⁺			H₃O·H₃O⁺	−4125.28342827	2.6
3.2	H₂O·H₃O⁺	H₃O⁺			H₃O⁺	−4125.28540851	1.4
3.5		H₂O·H₃O⁺	H₃O⁺	H₃O⁺		−4125.28756730	

^{a}Positions refer to previous table, and some more structures are added here. SVP basis and B3LYP functional are used.
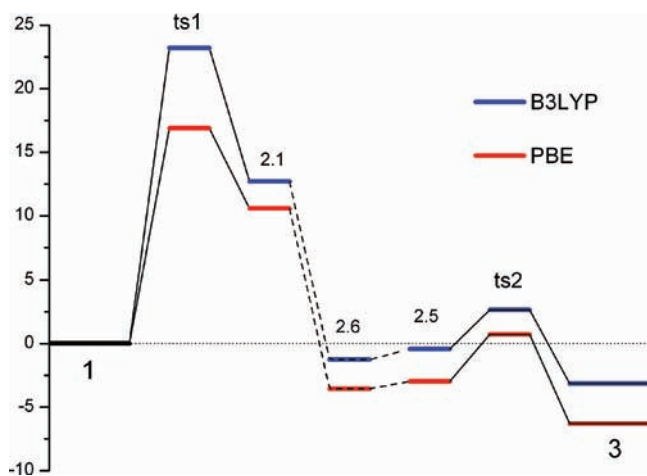
Figure 5. Reaction profile of Scheme 3 (energy in kcal/mol).

Finally the energetic profile of the reaction of Scheme 3 is shown in Figure 5 only for the equilibrium B3LYP and PBE data. This clearly shows the two step reaction mechanism described above, proceeding via the internal rearrangement between the two steps, as was extensively discussed earlier.

CONCLUSIONS

The protonation reaction of $[Mo_2Cl_8]^{4-}$ to produce the triply bridged $[Mo_2(\mu\text{-}H)(\mu\text{-}Cl)_2Cl_6]^{3-}$ hydride is fully elucidated using accurate quantum chemical calculations at the DFT level with a sufficiently large basis set.

From the computational point of view, there are two key conclusions to be mentioned. First, that a treatment without the explicit inclusion of solvent molecules, in this case $[H_3O]^+$, would lead to incorrect results, and that only when a reasonable number of solvent molecules is included in the immediate neighborhood of the central molecule the theoretical results agree with experiment. Second, a number of different DFT functionals, namely, B3LYP, PBE, and B97D, all produce broadly the same picture and similar results, giving confidence to the theoretical treatment.

From a chemical point of view, a classic reaction is examined in detail using modern theoretical techniques. Of great interest is the fact that although in their work Miller and Haim[9] correctly predict a two stage mechanism, suggesting that the second (rearrangement) and not the first (protonation of quadruple bond) is rate determining, theory clarifies this in depth and shows that this is not exactly the case. In particular, Miller and Haim had assumed that a protonated intermediate, where the proton would *not* be bridging the Mo—Mo bond, would be formed rapidly, followed by a slower rearrangement and formation of chloride and hydride bridges. They assumed that the formation of bridges, being a profound structural change as they say, would be slow. Theory shows that the formation of chloride bridges is fast, once the original protonation has taken place. The formation of the hydride bridge would also have been fast, had it not been for the presence of the solvent; it is this step, namely the transfer of the proton from the solvent to the Mo—Mo bond that the theoretical investigation finds to be the rate determining, with excellent agreement with experimental kinetic data.

Further investigations with the same methodology can be used to elucidate the mechanism of a great number of similar reactions.

ASSOCIATED CONTENT

Ⓢ Supporting Information

Reaction profile of Scheme 2 and relative energies for Scheme 3. This material is available free of charge via the Internet at http://pubs.acs.org.

AUTHOR INFORMATION

Corresponding Author

*E-mail msim@eie.gr.

Present Address

§Max-Planck Institut für Bioanorganische Chemie, Stiftstrasse 34-36, D-45470 Mülheim an der Ruhr, Germany.

REFERENCES

(1) (a) Huhmann-Vincent, J.; Scott, B. L.; Kubas, G. J. *Inorg. Chim. Acta* **1999**, *294* (2), 240−254. (b) Koelle, U. *New J. Chem.* **1992**, *16* (1−2), 157−169. (c) Quadrelli, E. A.; Kraatz, H. B.; Poli, R. *Inorg. Chem.* **1996**, *35* (18), 5154−5162.

(2) Stanbury, D. M., Reduction Potentials Involving Inorganic Free Radicals in Aqueous Solution. In *Advances in Inorganic Chemistry*; Sykes, A. G., Ed.; Academic Press: San Diego, CA, 1989; Vol. 33, pp 69−138.

(3) Harris, D. C.; Gray, H. B. *Inorg. Chem.* **1975**, *14* (5), 1215−1217.

(4) (a) Arabi, M. S.; Mathieu, R.; Poilblanc, R. *J. Organomet. Chem.* **1979**, *177* (1), 199−209. (b) Fauvel, K.; Mathieu, R.; Poilblanc, R. *Inorg. Chem.* **1976**, *15* (4), 976−978.

(5) Nataro, C.; Angelici, R. J. *Inorg. Chem.* **1998**, *37* (12), 2975−2983.

(6) (a) Amara, P.; Volbeda, A.; Fontecilla-Camps, J. C.; Field, M. J. *J. Am. Chem. Soc.* **1999**, *121* (18), 4468−4477. (b) De Gioia, L.; Fantucci, P.; Guigliarelli, B.; Bertrand, P. *Inorg. Chem.* **1999**, *38* (11), 2658−2662. (c) Niu, S. Q.; Thomson, L. M.; Hall, M. B. *J. Am. Chem. Soc.* **1999**, *121* (16), 4000−4007. (d) Pavlov, M.; Siegbahn, P. E. M.; Blomberg, M. R. A.; Crabtree, R. H. *J. Am. Chem. Soc.* **1998**, *120* (3), 548−555.

(7) Barton, B. E.; Rauchfuss, T. B. *Inorg. Chem.* **2008**, *47* (7), 2261−2263.

(8) Cotton, F. A.; Leung, P. C. W.; Roth, W. J.; Schultz, A. J.; Williams, J. M. *J. Am. Chem. Soc.* **1984**, *106* (1), 117−120.

(9) Miller, S. S.; Haim, A. *J. Am. Chem. Soc.* **1983**, *105* (17), 5624−5626.

(10) Takagi, N.; Krapp, A.; Frenking, G. *Can. J. Chem.* **2010**, *88* (11), 1079−1093.

(11) (a) Poineau, F.; Gagliardi, L.; Forster, P. M.; Sattelberger, A. P.; Czerwinski, K. R. *Dalton Trans.* **2009**, *30*, 5954−5959. (b) Ferrante, F.; Gagliardi, L.; Bursten, B. E.; Sattelberger, A. P. *Inorg. Chem.* **2005**, *44* (23), 8476−8480.

(12) Norman, J. G.; Kolari, H. J. *J. Am. Chem. Soc.* **1975**, *97* (1), 33−37.

(13) Brencic, J. V.; Cotton, F. A. *Inorg. Chem.* **1970**, *9* (2), 346−&.

(14) Tomasi, J.; Mennucci, B.; Cammi, R. *Chem. Rev.* **2005**, *105* (8), 2999−3093.

(15) Hush, N. S.; Schamberger, J.; Bacskay, G. B. *Coord. Chem. Rev.* **2005**, *249* (3−4), 299−311.

(16) Jaque, P.; Marenich, A. V.; Cramer, C. J.; Truhlar, D. G. *J. Phys. Chem. C* **2007**, *111* (15), 5783−5799.

(17) (a) Becke, A. D. *Phys. Rev. A* **1988**, *38* (6), 3098−3100. (b) Lee, C. T.; Yang, W. T.; Parr, R. G. *Phys. Rev. B* **1988**, *37* (2), 785−789.

(18) (a) Perdew, J. P.; Burke, K.; Ernzerhof, M. *Phys. Rev. Lett.* **1996**, *77* (18), 3865−3868. (b) Perdew, J. P.; Burke, K.; Ernzerhof, M. *Phys. Rev. Lett.* **1997**, *78* (7), 1396−1396.

(19) Grimme, S. *J. Comput. Chem.* **2006**, *27* (15), 1787−1799.

(20) Frisch, M. J.; G. W. T., H. B. Schlegel, G. E. Scuseria, M. A. Robb, J. R. Cheeseman, G. Scalmani, V. Barone, B. Mennucci, G. A. Petersson, H. Nakatsuji, M. Caricato, X. Li, H. P. Hratchian, A. F. Izmaylov, J. Bloino, G. Zheng, J. L. Sonnenberg, M. Hada, M. Ehara, K. Toyota, R. Fukuda, J. Hasegawa, M. Ishida, T. Nakajima, Y. Honda, O.

Kitao, H. Nakai, T. Vreven, J. A. Montgomery, Jr., J. E. Peralta, F. Ogliaro, M. Bearpark, J. J. Heyd, E. Brothers, K. N. Kudin, V. N. Staroverov, R. Kobayashi, J. Normand, K. Raghavachari, A. Rendell, J. C. Burant, S. S. Iyengar, J. Tomasi, M. Cossi, N. Rega, J. M. Millam, M. Klene, J. E. Knox, J. B. Cross, V. Bakken, C. Adamo, J. Jaramillo, R. Gomperts, R. E. Stratmann, O. Yazyev, A. J. Austin, R. Cammi, C. Pomelli, J. W. Ochterski, R. L. Martin, K. Morokuma, V. G. Zakrzewski, G. A. Voth, P. Salvador, J. J. Dannenberg, S. Dapprich, A. D. Daniels, Ö. Farkas, J. B. Foresman, J. V. Ortiz, J. Cioslowski., Fox, D. J. *Gaussian 09*, revision A.1; Gaussian, Inc.: Wallingford, CT, 2009.

(21) Weigend, F.; Ahlrichs, R. *Phys. Chem. Chem. Phys.* **2005**, 7 (18), 3297−3305.

(22) Andrae, D.; Haussermann, U.; Dolg, M.; Stoll, H.; Preuss, H. *Theor. Chim. Acta* **1990**, 77 (2), 123−141.

(23) Clark, R. J. H.; Franks, M. L. *J. Chem. Soc., Chem. Commun.* **1974**, 9, 316−317.

(24) Katovic, V.; McCarley, R. E. *Inorg. Chem.* **1978**, 17 (5), 1268−1270.

(25) Bino, A.; Bursten, B. E.; Cotton, F. A.; Fang, A. *Inorg. Chem.* **1982**, 21 (10), 3755−3759.

(26) Phillips, A. D.; Ienco, A.; Reinhold, J.; Böttcher, H.-C.; Mealli, C. *Chem.—Eur. J.* **2006**, 12 (17), 4691−4701.

(27) Mertis, C. C., M.; Chorianopoulou, M.; Koinis, S.; Psaroudakis, N. Homogeneous catalytic hydrogen formation using dinuclear multiply bonded complexes of molybdenum(III) and tungsten(III) and low valency metal ions M = Cr(II), V(II) in aqueous acidic solutions. In *Properties and Chemistry of Biomolecular Systems*; Russo, N., Ed.; Kluwer Academic Press: Dordrecht, The Netherlands, 1994; pp 321−329.